ISSN 1990-7931, Russian Journal of Physical Chemistry B, 2010, Vol. 4, No. 4, pp. 634–640. © Pleiades Publishing, Ltd., 2010.
Original Russian Text © V.Ya. Basevich, A.A. Belyaev, S.M. Frolov, 2010, published in Khimicheskaya Fizika, 2010, Vol. 29, No. 7, pp. 71–78.

COMBUSTION, EXPLOSION, AND SHOCK WAVES

Mechanisms of the Oxidation and Combustion of Normal Alkanes: Transition from C_1–C_5 to C_6H_{14}

V. Ya. Basevich, A. A. Belyaev, and S. M. Frolov
Semenov Institute of Chemical Physics, Russian Academy of Sciences, Moscow, 119991 Russia
e-mail: basevich@chph.ras.ru
Received June 29, 2009

Abstract—A previously proposed algorithm of constructing optimal mechanisms of the low- and high-temperature oxidation and combustion of normal alkanes was applied to *n*-hexane. The proposed mechanism can be considered a nonempirical detailed mechanism, since all the constituent reactions have a solid kinetic substantiation. The mechanism features two main peculiarities: it contains no reactions of double oxygen addition (first to the peroxide radical and then to its isomerized form) and (2) involves no isomeric compounds and derivatives thereof. Application of the algorithm to *n*-hexane made it possible to create a new compact kinetic mechanism. The mechanism was demonstrated to correctly describe the multistage character of low-temperature self-ignition: the appearance of a cool and then a blue flame.

DOI: 10.1134/S1990793110040147

INTRODUCTION

Given that the oxidation and combustion of higher hydrocarbons involves a large number of intermediate molecules and radicals, the current detailed mechanisms of these processes typically consist of thousands of reactions. For example, the kinetic scheme for *n*-heptane contains 2300 reactions involving 650 species [1], whereas that for *n*-decane includes 3872 reactions with 715 components [2]. Despite a number of indisputable merits of such mechanisms, their use in multidimensional gasdynamics calculations, in particular, in determination of the characteristics of turbulent combustion is extremely time-consuming. In addition, such mechanism, having a number of limitations, cannot be considered comprehensive. Simple estimates show that, if all the isomers of the components involved and all possible chemical reactions thereof were taken into account, including the formation and consumption of polyaromatic compounds, fullerenes, soot particles, etc., the sizes of the schemes stated in [1, 2] could be far exceeded. Note also that there are no reliable data on the thermodynamic functions and rate constants for many key reactions. In addition, an examination of many published mechanisms shows that they are inapplicable to describing the multistage low-temperature oxidation of hydrocarbons, since they are incapable of reproducing the experimentally observed cool and blue flames [3].

Numerical simulations of multidimensional reactive flows frequently require not an exhaustive but an optimal kinetic mechanism, composed of key elementary steps capable of predicting the rate of the overall process and the concentrations of the main intermediate and final products. Such mechanisms, even rather compacts ones, retain the status of nonempirical detailed mechanisms, since all the elementary steps have a kinetic foundation. Thus, there is a way of a nonextensive construction of detailed reaction mechanisms for modeling the oxidation and combustion of hydrocarbons, mechanisms that impose limitations on the numbers of species and reactions, but retain the main pathways and elementary steps.

The oxidation and combustion of paraffin hydrocarbons are known to have much in common [3, 4]. In the present work, we applied the algorithm for constructing reaction mechanisms of the oxidation and combustion of alkanes formulated in [5] to *n*-hexane (C_6H_{14}). This algorithm is based on the principle of nonextensive construction of reaction mechanisms, which, in turn, rests on two assumptions: (1) low-temperature branching involves a set of reactions with one oxygen addition and (2) oxidation through isomerized forms, being slower that the oxidation through the analogous nonisomeric forms, is unimportant. Various mechanisms of C_6H_{14} oxidation have been proposed in a number of works, see, e.g., [6, 7]. Note, however, that these mechanisms, as those for the other aforementioned compounds, have not been demonstrated to adequately describe the multistage oxidation of C_6H_{14}, which manifests itself as cool and blue flames. The construction of a C_6H_{14} oxidation mechanism based on the principle of nonextensivity is a necessary and important step in developing oxidation mechanisms for higher hydrocarbons following this principle.

Table 1. Additional components included into the mechanism of n-hexane oxidation and combustion as it was built upon an analogous mechanism for n-pentane

Number of the component	Formula	$\Delta H^0_{f\,298}$, cal/mol	S^0_{298}, cal/mol K	c_0	c_1	c_2	c_3
64	C_6H_{14}	–0.396E+05	0.932E+02	0.365E–01	0.138E+03	–0.742E+02	0.156E+02
65	C_6H_{13}	0.860E+04	0.969E+02	0.167E+01	0.128E+03	–0.720E+02	0.181E+02
66	$C_6H_{13}O_2$	–0.191E+05	0.115E+03	0.250E+01	0.154E+03	–0.938E+02	0.268E+02
67	$C_6H_{14}O_2$	–0.548E+05	0.114E+03	0.218E+01	0.157E+03	–0.936E+02	0.262E+02
68	$C_6H_{13}O$	–0.213E+05	0.106E+03	–0.217E+00	0.153E+03	–0.953E+02	0.289E+02
69	$C_6H_{12}O$	–0.600E+05	0.101E+03	0.108E+02	0.882E+02	0.519E+01	–0.377E+02
70	$C_6H_{11}O$	–0.248E+05	0.103E+03	0.108E+02	0.882E+02	0.519E+01	–0.377E+02
71	C_6H_{12}	–0.992E+04	0.925E+02	0.197E+01	0.120E+03	–0.640E+02	0.132E+02
72	C_6H_{11}	0.342E+05	0.917E+02	0.258E+01	0.107E+03	–0.528E+02	0.101E+02

CONSTRUCTION OF THE MECHANISM

According to the algorithm used in [5], the core of the mechanism of the oxidation of a C_nH_{2n+2} hydrocarbon is the oxidation mechanism for its preceding analogue in the homologous series, $C_{n-1}H_{2(n-1)+2}$, regarding both the reactants and reactions. For n-hexane, the preceding analogue is n-pentane; therefore, the mechanism of n-hexane oxidation was based on the mechanism of the oxidation and combustion of n-C_5H_{12} [8]. It was composed of 387 reactions involving 63 components. To adapt, the kinetic mechanism for n-pentane to n-hexane, it was extended to include 9 new components and 112 new elementary reactions, so that the resultant mechanism for n-hexane consisted of 499 reactions involving 72 species. Tables 1 and 2 list the new components selected by the computational code [5] and their properties (enthalpy ΔH^0_{f298}, entropy S^0_{298} and heat capacity at constant pressure: $c_p = c_0 + c_1T/10^3 + c_2T^2/10^6 + c_3T^3/10^9$), as well as the new reactions and their Arrhenius parameters. Critical phenomena, including the emergence of cool and blue flames during multistage autoignition, are of multifunctional character and manifest themselves at certain ratios between the rate constants of the different elementary reactions. This means that the use of approximate values of the rate constants of the governing reactions not always provides the expected result. Therefore, in modeling critical phenomena, it is necessary to perform an additional analysis and selection of the rate constants within the theoretically admissible range and the experimental error limits. In the proposed kinetic mechanism of n-hexane oxidation, such a correction was applied to a limited number of reactions (the reactions of n-hexane with hydroperoxide radicals and the reaction of n-hexyl with molecular oxygen).

VALIDATION OF THE MECHANISM

The proposed kinetic mechanism was tested by simulating the characteristics of the oxidation and autoignition of n-C_6H_{14} reported in the literature. The calculations were performed using the standard kinetic code [5].

Simulation of the Experimental Results from the Works [7, 9]

Figure 1 shows typical calculated time histories of the temperature for the autoignition of a n-hexane–air mixture. At a high temperature (1190 K in Fig. 1), autoignition occurs as a one-stage process, with a

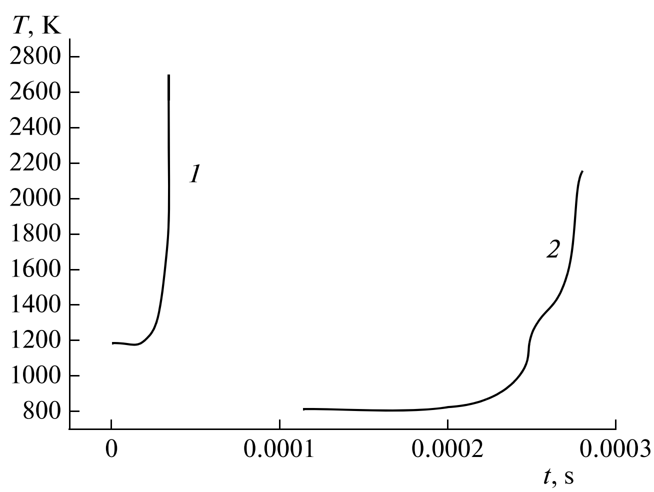

Fig. 1. Calculated time histories of the temperature for the self-ignition of a 1.08% C_6H_{14}–air mixture at initial temperatures of (*1*) 1190 and (*2*) 820 K and an initial pressure of 220 atm.

Table 2. Mechanism of the oxidation and combustion of *n*-hexane

Number of the reaction	Reaction	A, l, mol, s	E/R, K
1	$C_6H_{14} + O_2 = C_6H_{13} + HO_2$	0.400E+10	0.239E+05
2	$C_6H_{14} + OH = C_6H_{13} + H_2O$	0.630E+10	0.600E+03
3	$C_6H_{14} + H = C_6H_{13} + H_2$	0.930E+11	0.403E+04
4	$C_6H_{14} + O = C_6H_{13} + OH$	0.506E+12	0.483E+04
5	$C_6H_{14} + HO_2 = C_6H_{13} + H_2O_2$	0.600E+09	0.856E+04
6	$C_6H_{12} + H = C_6H_{13}$	0.189E+10	0.315E+03
7	$C_6H_{13} + O_2 = C_6H_{12} + HO_2$	0.220E+10	0.800E+04
8	$C_6H_{13} + OH = C_6H_{12} + H_2O$	0.600E+10	0.000E+00
9	$C_6H_{14} = H + C_6H_{13}$	0.359E+14	0.376E+05
10	$C_6H_{14} = CH_3 + C_5H_{11}$	0.404E+16	0.421E+05
11	$C_6H_{14} = C_2H_5 + C_4H_9$	0.195E+17	0.428E+05
12	$C_6H_{14} = C_3H_7 + C_3H_7$	0.157E+17	0.428E+05
13	$C_6H_{13} + H = C_6H_{12} + H_2$	0.600E+10	0.000E+00
14	$C_6H_{13} + CH_3 = C_6H_{12} + CH_4$	0.351E+09	−0.106E+03
15	$C_6H_{13} + C_2H_5 = C_6H_{12} + C_2H_6$	0.103E+09	0.466E+03
16	$C_6H_{13} + C_3H_7 = C_6H_{12} + C_3H_8$	0.138E+09	0.488E+03
17	$C_6H_{13} + C_4H_9 = C_6H_{12} + C_4H_{10}$	0.138E+09	0.488E+03
18	$C_6H_{13} + C_5H_{11} = C_6H_{12} + C_5H_{12}$	0.138E+09	0.488E+03
19	$C_6H_{13} + O = C_6H_{12} + OH$	0.200E+12	0.000E+00
20	$C_6H_{13} + O_2 = C_6H_{13}O_2$	0.400E+08	−0.500E+03
21	$C_6H_{14} + CH_3O_2 = C_6H_{13} + CH_3O_2H$	1.000E+10	0.650E+04
22	$C_6H_{14} + C_2H_5O_2 = C_6H_{13} + C_2H_5O_2H$	1.000E+10	0.650E+04
23	$C_6H_{14} + C_3H_7O_2 = C_6H_{13} + C_3H_7O_2H$	1.000E+10	0.650E+04
24	$C_6H_{14} + C_4H_9O_2 = C_6H_{13} + C_4H_{10}O_2$	1.000E+10	0.650E+04
25	$C_6H_{14} + C_5H_{11}O_2 = C_6H_{13} + C_5H_{12}O_2$	1.000E+10	0.650E+04
26	$C_6H_{14} + C_6H_{13}O_2 = C_6H_{13} + C_6H_{14}O_2$	1.000E+09	0.650E+04
27	$C_6H_{14}O_2 = C_6H_{13}O + OH$	0.499E+16	0.200E+05
28	$C_6H_{13}O = H_2CO + C_5H_{11}$	0.158E+15	0.797E+04
29	$C_6H_{13}O = CH_3CHO + C_4H_9$	0.312E+15	0.113E+05
30	$C_6H_{13}O = C_2H_5CHO + C_3H_7$	0.302E+15	0.103E+05
31	$C_6H_{13}O = C_4H_8O + C_2H_5$	0.374E+15	0.103E+05
32	$C_6H_{13}O = C_5H_{10}O + CH_3$	0.775E+14	0.108E+05
33	$C_6H_{13}O = C_6H_{12}O + H$	0.688E+12	0.626E+04
34	$C_6H_{13}O_2 + H = C_6H_{13}O + OH$	0.236E+11	−0.161E+04
35	$C_6H_{13}O_2 + CH_3 = C_6H_{13}O + CH_3O$	0.364E+09	−0.166E+03
36	$C_6H_{13}O_2 + C_2H_5 = C_6H_{13}O + C_2H_5O$	0.826E+09	−0.649E+03
37	$C_6H_{13}O_2 + C_3H_7 = C_6H_{13}O + C_3H_7O$	0.629E+09	0.000E+00
38	$C_6H_{13}O_2 + C_4H_9 = C_6H_{13}O + C_4H_9O$	0.629E+09	0.000E+00
39	$C_6H_{13}O_2 + C_5H_{11} = C_6H_{13}O + C_5H_{11}O$	0.629E+09	0.000E+00
40	$C_6H_{13}O_2 + C_6H_{13} = C_6H_{13}O + C_6H_{13}O$	0.629E+09	0.000E+00
41	$C_6H_{13}O_2 + H_2CO = C_6H_{14}O_2 + HCO$	0.320E+09	0.564E+04
42	$C_6H_{13}O_2 + CH_3CHO = C_6H_{14}O_2 + CH_3CO$	0.315E+09	0.560E+04
43	$C_6H_{13}O_2 + C_2H_5CHO = C_6H_{14}O_2 + C_2H_5CO$	0.315E+09	0.554E+04
44	$C_6H_{13}O_2 + C_4H_8O = C_6H_{14}O_2 + C_4H_7O$	0.315E+09	0.554E+04
45	$C_6H_{13}O_2 + C_5H_{10}O = C_6H_{14}O_2 + C_5H_9O$	0.315E+09	0.554E+04
46	$C_6H_{13}O_2 + C_6H_{12}O = C_6H_{14}O_2 + C_6H_{11}O$	0.315E+09	0.554E+04
47	$C_6H_{13} + HO_2 = C_6H_{13}O + OH$	0.300E+11	0.000E+00
48	$C_6H_{13} + O_2 = C_6H_{12}O + OH$	0.400E+10	0.900E+04
49	$C_6H_{13} + C_2H_5 = C_6H_{14} + C_2H_4$	0.625E+09	0.335E+03
50	$C_6H_{13} + C_3H_7 = C_6H_{14} + C_3H_6$	0.190E+10	0.000E+00
51	$C_6H_{13} + C_4H_9 = C_6H_{14} + C_4H_8$	0.190E+10	0.000E+00
52	$C_6H_{13} + C_5H_{11} = C_6H_{14} + C_5H_{10}$	0.190E+10	0.000E+00
53	$C_6H_{13} + C_6H_{13} = C_6H_{14} + C_6H_{12}$	0.190E+10	0.000E+00
54	$C_6H_{13} + O_2 = H_2CO + C_5H_{11}O$	0.400E+09	0.700E+04
55	$C_6H_{13} + O_2 = CH_3CHO + C_4H_9O$	0.400E+09	0.700E+04
56	$C_6H_{13} + O_2 = C_2H_5CHO + C_3H_7O$	0.400E+09	0.700E+04
57	$C_6H_{13} + O_2 = C_4H_8O + C_2H_5O$	0.400E+10	0.700E+04
58	$C_6H_{13} + O_2 = C_5H_{10}O + CH_3O$	0.400E+09	0.700E+04

Table 2. (Contd.)

Number of the reaction	Reaction	A, l, mol, s	E/R, K
59	$C_6H_{13} + OH = CH_3 + C_5H_{11}O$	0.185E+11	–0.194E+04
60	$C_6H_{13} + OH = C_2H_5 + C_4H_9O$	0.891E+11	0.417E+03
61	$C_6H_{13} + OH = C_3H_7 + C_3H_7O$	0.719E+11	0.413E+03
62	$C_6H_{13} + OH = C_4H_9 + C_2H_5O$	0.117E+12	–0.232E+03
63	$C_6H_{13} + OH = C_5H_{11} + CH_3O$	0.107E+11	0.480E+03
64	$C_6H_{13} + H = CH_3 + C_5H_{11}$	0.388E+11	0.546E+03
65	$C_6H_{13} + H = C_2H_5 + C_4H_9$	0.187E+12	0.318E+03
66	$C_6H_{13} + H = C_3H_7 + C_3H_7$	0.151E+12	0.314E+03
67	$C_6H_{13} + H = CH_2 + C_5H_{12}$	0.649E+10	0.302E+04
68	$C_6H_{13} + H = C_2H_4 + C_4H_{10}$	0.111E+10	–0.641E+04
69	$C_6H_{13} + H = C_3H_6 + C_3H_8$	0.272E+10	–0.675E+04
70	$C_6H_{13} + H = C_4H_8 + C_2H_6$	0.251E+10	–0.677E+04
71	$C_6H_{13} + H = C_5H_{10} + CH_4$	0.178E+10	–0.711E+04
72	$C_6H_{13} + O = H + C_6H_{12}O$	0.702E+09	0.565E+03
73	$C_6H_{13} + O = CH_3 + C_5H_{10}O$	0.791E+11	–0.952E+03
74	$C_6H_{13} + O = C_2H_5 + C_4H_8O$	0.381E+12	–0.118E+04
75	$C_6H_{13} + O = C_3H_7 + C_2H_5CHO$	0.308E+12	–0.118E+04
76	$C_6H_{13} + O = C_4H_9 + CH_3CHO$	0.318E+12	–0.111E+04
77	$C_6H_{13} + O = C_5H_{11} + H_2CO$	0.162E+12	–0.352E+01
78	$C_6H_{11}O + HO_2 = C_6H_{12}O + O_2$	0.530E+08	0.000E+00
79	$C_6H_{12}O + OH = C_6H_{11}O + H_2O$	0.100E+11	0.000E+00
80	$C_6H_{12}O + H = C_6H_{11}O + H_2$	0.140E+11	0.165E+04
81	$C_6H_{12}O + O = C_6H_{11}O + OH$	0.568E+10	0.780E+03
82	$C_6H_{12}O + HO_2 = C_6H_{11}O + H_2O_2$	0.600E+09	0.500E+04
83	$C_5H_{11} + HCO = C_6H_{12}O$	0.223E+11	0.352E+01
84	$C_5H_{11} + CO = C_6H_{11}O$	0.187E+09	0.242E+04
85	$C_6H_{11}O + H = C_5H_{11} + HCO$	0.485E+10	0.240E+04
86	$C_6H_{11}O + O = C_5H_{11}O + CO$	0.369E+10	0.646E+03
87	$C_6H_{12} + OH = C_6H_{11} + H_2O$	0.900E+11	0.325E+04
88	$C_6H_{11} + H_2 = C_6H_{12} + H$	0.853E+11	0.533E+04
89	$C_6H_{11} + O_2 = C_4H_9O_2 + C_2H_2$	0.242E+11	0.396E+04
90	$C_6H_{12} + HCO = C_6H_{11} + H_2CO$	0.600E+11	0.900E+04
91	$C_6H_{12} + CH_3 = C_6H_{11} + CH_4$	0.107E+09	0.268E+04
92	$C_6H_{12} + C_2H_5 = C_6H_{11} + C_2H_6$	0.313E+08	0.325E+04
93	$C_6H_{12} + C_3H_7 = C_6H_{11} + C_3H_8$	0.420E+08	0.328E+04
94	$C_6H_{12} + C_4H_9 = C_6H_{11} + C_4H_{10}$	0.420E+08	0.328E+04
95	$C_6H_{12} + C_5H_{11} = C_6H_{11} + C_5H_{12}$	0.420E+08	0.328E+04
96	$C_4H_9 + C_2H_2 = C_6H_{11}$	0.141E+10	0.143E+04
97	$C_6H_{12} = C_2H_3 + C_4H_9$	0.390E+14	0.379E+05
98	$C_6H_{12} = C_3H_5 + C_3H_7$	0.113E+14	0.446E+05
99	$C_6H_{12} = C_4H_7 + C_2H_5$	0.140E+14	0.446E+05
100	$C_6H_{12} = C_5H_9 + CH_3$	0.289E+13	0.439E+05
101	$C_6H_{12} + O_2 = C_6H_{11} + HO_2$	0.600E+11	0.236E+05
102	$C_6H_{12} + O = C_5H_{11} + HCO$	0.404E+10	0.226E+03
103	$C_6H_{11} + OH = C_5H_{11} + HCO$	0.485E+10	–0.352E+01
104	$C_6H_{11} + H = C_4H_{10} + C_2H_2$	0.917E+10	0.362E+03
105	$C_6H_{11} + O = C_5H_{11} + CO$	0.485E+10	–0.352E+01
106	$C_6H_{11} + O = C_4H_9O + C_2H_2$	0.405E+11	–0.662E+02
107	$CH_3 + C_5H_{11} = C_6H_{12} + H_2$	0.248E+14	0.191E+05
108	$C_2H_5 + C_4H_9 = C_6H_{12} + H_2$	0.513E+13	0.193E+05
109	$C_3H_7 + C_3H_7 = C_6H_{12} + H_2$	0.636E+13	0.193E+05
110	$C_4H_9 + C_2H_5 = C_6H_{12} + H_2$	0.513E+13	0.193E+05
111	$C_6H_{12} + H + H = CH_3 + C_5H_{11}$	0.356E+10	–0.500E+04
112	$C_6H_{12} + H + H = C_2H_5 + C_4H_9$	0.172E+11	–0.523E+04
113	$C_6H_{12} + H + H = C_3H_7 + C_3H_7$	0.139E+11	–0.524E+04
114	$C_6H_{12} + H + H = C_4H_9 + C_2H_5$	0.172E+11	–0.523E+04

(what follows is the mechanism of the oxidation and combustion of C_1–C_5)

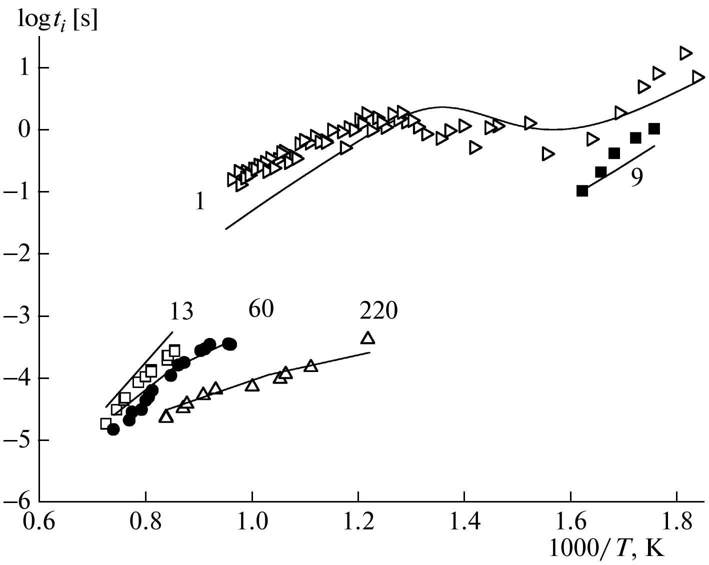

Fig. 2. Calculated (lines) and measured (symbols) temperature dependences of the ignition delay times for two *n*-hexane–air mixtures at various pressures: the lower group of points refers to a 1.08% C_6H_{14}–air mixture at initial pressures of 13, 60, and 220 atm [7], whereas the upper group to a 2.15% C_6H_{14}–air mixture at initial pressures of 1 and 9 atm [8].

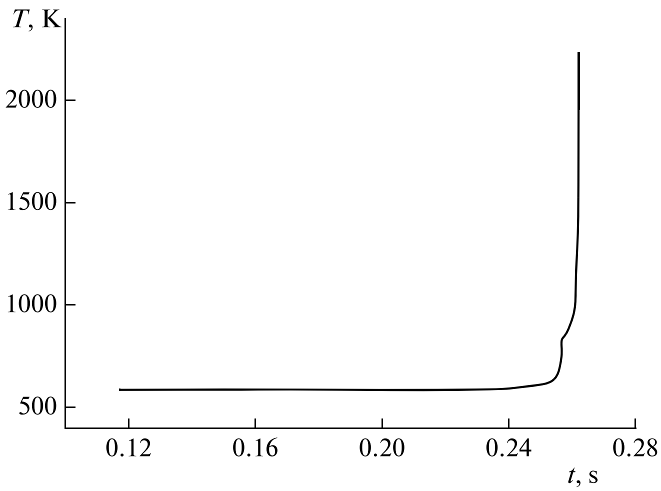

Fig. 3. Calculated time profile of the temperature for the self-ignition of a 3.53% C_6H_{14}–air mixture at an initial temperature of 593 K and an initial pressure of 5 atm.

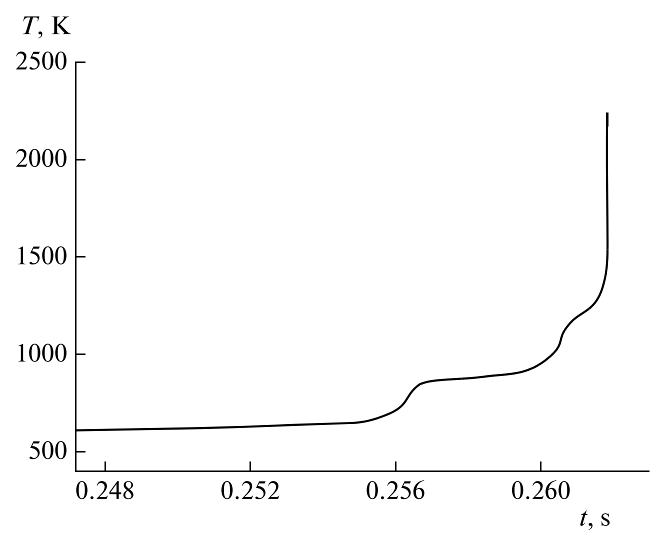

Fig. 4. The same as in Fig. 3 but at a higher time resolution.

smooth, nearly exponential temperature rise. At a lower temperature (820 K in Fig. 1), autoignition occurs as a two-stage process, with the first stage corresponding to the emergence of a cool flame. Figure 2 compares the calculated (curves) and measured temperature dependences of the ignition delay time at various pressures and fuel-to-oxidizer equivalence ratios: $P_0 = 13$, 60, and 220 atm and $f = 0.5$ [7] and $P_0 = 1$ and 9 atm and $f = 1.0$ [9]. As can be seen, the calculation and experimental results are in satisfactory agreement.

Simulation of the Experimental Results from the Work [10]

Figure 3 displays a typical calculated time history of the temperature for the autoignition of a *n*-hexane–air mixture for the pressure and temperature range covered in the experiments reported in [10]. The temperature rise in Fig. 3 looks as proceeding in two stages, but in fact, it occurs in three stages, as can be seen at a higher time resolution (Fig. 4). The first temperature rise step, associated with the emergence of a cool flame, is located at a time of $t \sim 0.256$ s. The second step, related to the appearance of a blue flame, is posi-

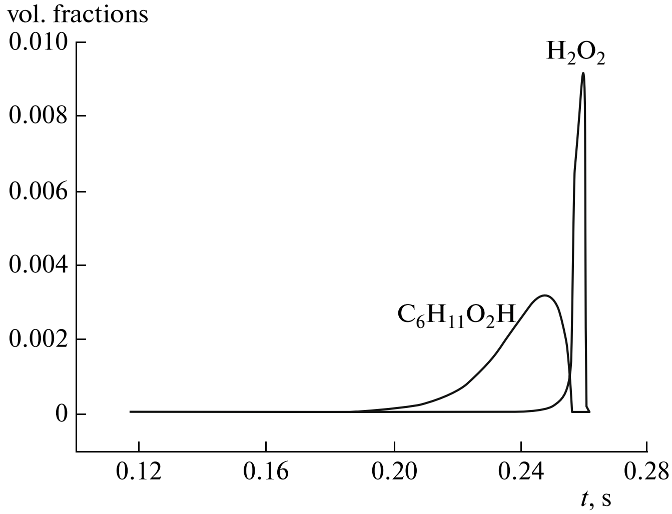

Fig. 5. Calculated time dependences of the concentrations of peroxides for the self-ignition of a 3.53% C_6H_{14}–air mixture at an initial temperature of 593 K and an initial pressure of 5 atm.

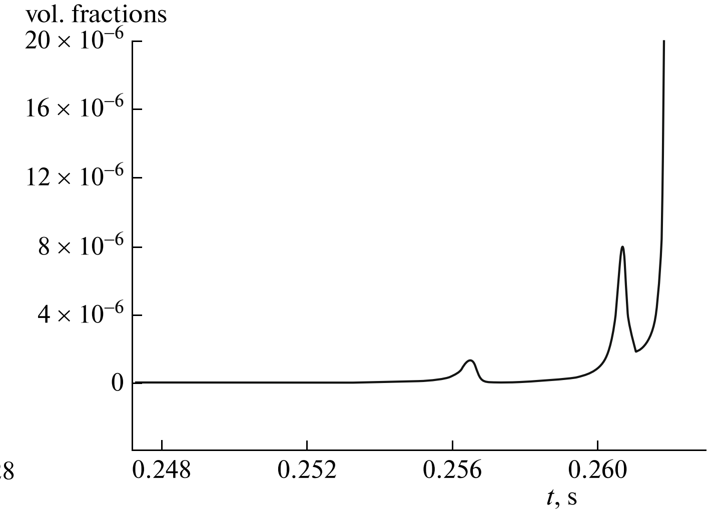

Fig. 6. Calculated time dependence of the concentration of hydroxyl radicals for the self-ignition of a 3.53% C_6H_{14}–air mixture at an initial temperature of 593 K and an initial pressure of 5 atm.

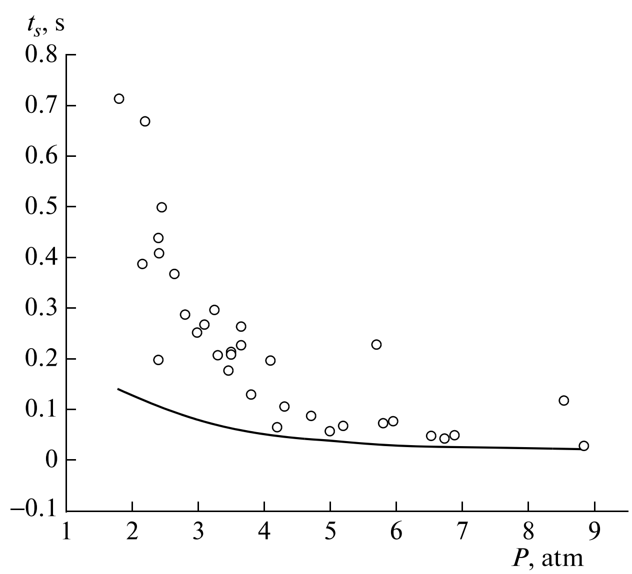

Fig. 7. Comparison of the calculated (curves) and measured (symbols) pressure dependences of the ignition delay times for the self-ignition of a 3.53% C_6H_{14}–air mixture at an initial temperature of 653–673 K.

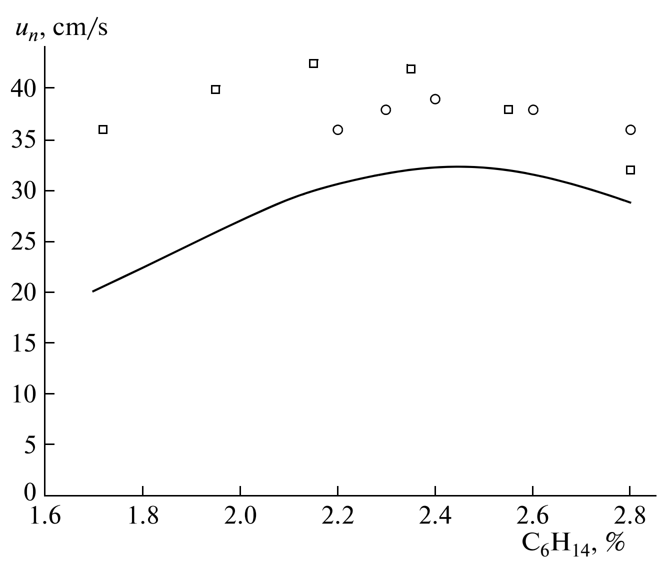

Fig. 8. Comparison of the calculated (curve) and measured (circles from [12] and squares from [13]) dependences of the laminar flame speed on the fuel concentration in the *n*-hexane–air mixture at atmospheric pressure and an initial temperature of 293 K.

tion at $t \sim 0.260$ s. At $t \sim 0.262$ s, a hot flame arises, with the temperature rapidly increasing to the combustion temperature. This sequence of events manifests the multistage character of self-ignition: the consecutive appearance of a cool, blue, and hot flame. The acceleration of the reaction in the cool flame is a consequence of the chain branching reaction of alkyl hydroperoxide (hexyl hydroperoxide in our case) decomposition. The blue flame arises due to the chain branching reaction associated with hydrogen peroxide decomposition. This conclusion follows from an analysis of the kinetic curves for these peroxides and two hydroxyl concentration peaks in Figs. 5 and 6. In experiments, such a separation of the stages was not always noticeable, possibly due to temperature nonuniformities.

Figure 7 compares the measured [10] and calculated (present work) temperature ignition delay times at initial temperatures of $T_0 = 653$–673 K and various pressures.

Simulation of the Experimental Results on Flame Propagation

We also compared the results of our calculations (computational code from [11]) of the laminar flame speed u_n in a n-hexane–air mixture (at atmospheric pressure and $T_0 = 293$ K) with the experimental data from [12, 13] (Fig. 8). As can be seen, a satisfactory agreement is observed.

CONCLUSIONS

The results of kinetic calculations and the available experimental data on the self-ignition and combustion of n-hexane–air mixtures were found to be in satisfactory qualitative and quantitative agreement with each other. The principle underlying the algorithm developed in [5] and the new kinetic mechanism of C_6H_{14} oxidation and combustion constructed based on it can be used for creating detailed kinetic mechanisms for higher paraffin hydrocarbons.

ACKNOWLEDGMENTS

This work was supported by the Russian Foundation for Basic Research, project nos. 08-08-00068 and 07-08-00558.

REFERENCES

1. C. Chevalier, P. Louessard, U. C. Muller, and J. Warnatz, in *Proc. of the Joint Meeting, Sov.-Ital. Sections Comb. Inst.* (The Combust. Inst., Pisa, 1990), p. 5.
2. F. Buda, R. Bounaceur, V. Warth, et al., Combust. Flame **142**, 170 (2005).
3. A. S. Sokolik, *Self-Ignition, Flame and Detonation in Gases* (Akad. Nauk SSSR, Moscow, 1960) [in Russian].
4. B. Lewis and G. Elbe, *Combustion, Flames and Explosions of Gases* (Acad. Press, Orlando, 1987).
5. V. Ya. Basevich, A. A. Belyaev, and S. M. Frolov, Khim. Fiz. **26** (7), 37 (2007) [Russ. J. Phys. Chem. B **26**, 477 (2007)].
6. J. Warnatz, in *Proc. 20th Intern. Symp. on Combustion* (Combust. Inst., Pittsburghs, 1984), p. 845.
7. V. P. Zhukov, V. A. Sechenov, and A. Yu. Starikovskii, Combust. Flame **136**, 257 (2004).
8. V. Ya. Basevich, A. A. Belyaev, and S. M. Frolov, Khim. Fiz. **28** (8), 59 (2009) [Russ. J. Phys. Chem. B **28**, 629 (2009)].
9. K. Ya. Troshin, Khim. Fiz. **27** (6), 6 (2008) [Russ. J. Phys. Chem. B **27**, 419 (2008)].
10. A. S. Kravets, A. S. Sokolik, and S. A. Yantovskii, Zh. Fiz. Khim. **13**, 1742 (1939).
11. A. A. Belyaev and V. S. Posvyanskii, "Algorithms and Programs," Inform. Bull. Gos. Fonda Algoritmov Programm SSSR, No. 3, 35 (1985).
12. M. Gerstein, O. Levin, and E. L. Wang, J. Am. Chem. Soc. **73**, 418 (1951).
13. G. J. Gibbs and H. F. Calcote, J. Chem. Eng. Data **4**, 226 (1959).